

# Molecular properties of pyruvate bound to lactate dehydrogenase: A Raman spectroscopic study

(substrate/bond orders/carbonyls/ion pairs)

HUA DENG\*, JIE ZHENG\*, JOHN BURGNER<sup>†‡</sup>, AND ROBERT CALLENDER\*<sup>‡</sup>

\*Physics Department, City College of the City University of New York, New York, NY 10031; and <sup>†</sup>Department of Biological Sciences, Purdue University, West Lafayette, IN 47907

Communicated by William Jencks, February 13, 1989 (received for review November 21, 1988)

**ABSTRACT** Lactate dehydrogenase (LDH; EC 1.1.1.27) catalyzes the addition of pyruvate to the four position of the nicotinamide ring of bound NAD<sup>+</sup>; this NAD-pyruvate adduct is bound tightly to the enzyme. We have used the adduct as a model for pyruvate in a competent ternary complex by comparing the Raman spectrum of the bound adduct with that for unliganded pyruvate. To understand the observed normal modes of pyruvate both as the bound adduct and in water, we have taken the Raman spectra of a series of <sup>13</sup>C- and <sup>18</sup>O-labeled pyruvates. We find that the carboxylate COO<sup>-</sup> moiety of pyruvate remains unprotonated at LDH's active site and forms an ion pair complex. The frequency of pyruvate's carbonyl C=O moiety shifts from 1710 cm<sup>-1</sup> in water downward 34 cm<sup>-1</sup> when pyruvate binds to LDH. This frequency shift corresponds to a ca. 34% polarization of the carbonyl bond, indicates a substantial interaction between the C=O group and enzyme, and is direct evidence for and is a measure of enzyme-induced electronic perturbation of the substrate needed for catalysis. This bond polarization is likely brought about by electrostatic interactions between the carbonyl moiety and the protonated imidazole group of His-195 and the guanidino group from Arg-109. We discuss how the data bear on the enzymatic chemistry of LDH.

Typically, there are specific molecular interactions between a substrate and enzyme, which occur during catalysis, that must be sufficient to not only reduce the transition state barrier appropriate for the reaction but also define the specificity of the enzyme (1-3). Both the origins and strengths of these interactions are fundamental issues in understanding how enzymes work. Although more structural information is increasingly available from x-ray crystallographic studies, the extent of these interactions and the electronic character of the substrate and nearby protein groups within the active site generally must be simply surmised from the structural data and kinetic studies. Rarely are these molecular properties directly measured. We have approached this problem by determining the vibrational spectra of bound substrates using Raman spectroscopy. The observed vibrational frequencies are a measure of force constants between particular atoms, and these constants can be related in turn to bond orders and electronic distributions between these atoms.

Lactate dehydrogenase (LDH; EC 1.1.1.27) accelerates the oxidation of lactate by NAD<sup>+</sup> to pyruvate and NADH by about 10<sup>14</sup>-fold (4) according to Scheme I (where ADPR indicates adenosine 5'-diphosphate ribose). This reversible reaction involves the direct transfer of a hydride ion, H<sup>-</sup>, from the pro-R face of NADH to the C2 carbon of pyruvate forming L-lactate and NAD<sup>+</sup> with a degree of fidelity approaching 100% (5).

We are able to study pyruvate bound to LDH by determining the Raman spectrum of an adduct formed by the addition of the C3 carbon of *enol*pyruvate to the C4 position of the nicotinamide ring of NAD<sup>+</sup> in the presence of LDH (4, 6). The enzyme also accelerates this reaction at a significant rate (10<sup>11</sup>-fold). This adduct, NAD-pyruvate (NAD-pyr), which has a dihydro-like nicotinamide ring, is bound tightly to the enzyme ( $K_d = 10^{11} \text{ M}^{-1}$ ). Based on x-ray structural evidence (7-9) and chemical studies (4, 6), the pyruvate moiety of the adduct interacts with the same residues that interact with oxamate in the E/NADH/oxamate ternary complex and that are proposed to interact with pyruvate in its central complex with LDH.

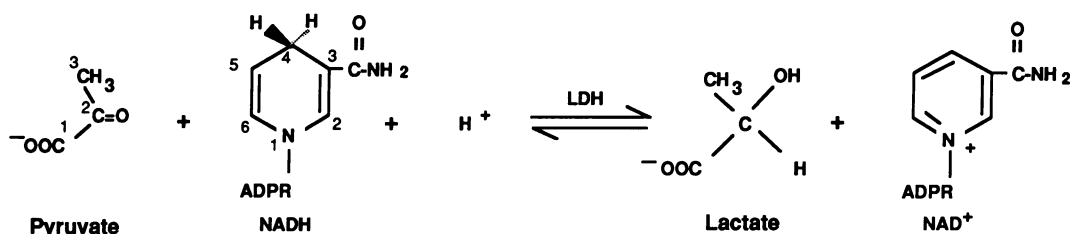
The Raman spectrum of the bound NAD-pyr enzyme adduct is obtained by subtracting the spectrum of LDH from the enzyme adduct complex using the subtraction procedures that we have developed previously (10, 11). These procedures are accurate, and differences of as little as 0.3% can be detected. The resulting difference spectrum can have contributions from the bound pyruvate moiety, from the remaining parts of the adduct, which is NADH-like, and from disturbed protein moieties. To identify bands arising from bound pyruvate and to help determine the normal mode character of the observed bands, we obtain difference spectra from <sup>18</sup>O- and <sup>13</sup>C-labeled pyruvate. We also report on the spectra of pyruvate and its isotopically labeled analogs in solution for comparison purposes. Pyruvate, rather than the unbound pyruvate adduct, must be used since the adduct cyclizes in the absence of enzyme.

We are able to address several issues concerning the enzymatic chemistry of LDH with this data. Our results below show that the carbonyl C=O bond is strongly polarized, which results in a much reduced bond order and concomitant vibrational frequency. Thus, a substantial positive charge must accumulate on the C2 carbon, which clearly facilitates the attack of a hydride ion on this atom. Moreover, the polar transition state associated with the pyruvate to lactate transition would be substantially stabilized. This bond polarization is brought about by electrostatic interactions between pyruvate's carbonyl moiety and the protein that probably involve the imidazole ring of His-195 and the guanidino group of Arg-109, as judged from the x-ray results. We find also that the carboxylate of pyruvate is unprotonated at the active site and likely forms a strongly interacting ion pair with Arg-171. We contrast these results with previous results on an aldehyde substrate bound to the active site of liver alcohol dehydrogenase (LADH). In this enzyme, where Zn<sup>2+</sup> polarizes the carbonyl of the substrate analog (12), we also found a strong carbonyl bond polarization, although the

The publication costs of this article were defrayed in part by page charge payment. This article must therefore be hereby marked "advertisement" in accordance with 18 U.S.C. §1734 solely to indicate this fact.

Abbreviations: LDH, lactate dehydrogenase; NAD-pyr, NAD-pyruvate; DABA, *p*-(dimethylamino)benzaldehyde; LADH, liver alcohol dehydrogenase.

<sup>‡</sup>To whom reprint requests should be addressed.



molecular environment around the substrate is entirely different than in LDH.

## MATERIALS AND METHODS

NAD<sup>+</sup> (100%) was purchased from Boehringer Mannheim; sodium pyruvate (type II, 99%) was purchased from Sigma; sodium [1-<sup>13</sup>C]pyruvate, sodium [2-<sup>13</sup>C]pyruvate, and sodium [3-<sup>13</sup>C]pyruvate (99% <sup>13</sup>C) were purchased from MSD Isotopes (Montreal); H<sub>2</sub><sup>18</sup>O (95%) was purchased from Monsanto Research (Miamisburg, OH); and they were used without further purification. Pig H<sub>4</sub> LDH was prepared according to the procedure described in Burgner and Ray (4) and stored at 4°C in 2.6 M ammonium sulfate/0.1 M phosphate, pH 7.2. Before use, LDH was dialyzed against 0.1 M phosphate buffer at pH 7.2 and 4°C for several hours. After removing insoluble protein by centrifugation, the enzyme solution was concentrated to about 1 mM, corresponding to a binding site concentration of 4 mM, using a centricon centrifuge concentrator (Amicon). The enzyme activity was measured before and after each Raman experiment; no significant activity loss was detected. Concentrations of enzyme and coenzymes were determined by UV-visible absorption spectroscopy, using  $\epsilon_{280} = 200,000 \text{ M}^{-1}\text{cm}^{-1}$  for LDH and  $\epsilon_{259} = 18,000 \text{ M}^{-1}\text{cm}^{-1}$  for NAD<sup>+</sup>. Since LDH contains four independent active sites, LDH/NAD-pyr complexes were prepared by mixing a 1:2:2.5 molar ratio of LDH to NAD<sup>+</sup> to pyruvate. Under these conditions, virtually all of the NAD<sup>+</sup> will be bound to the enzyme (13, 14). Unbound pyruvate was not observed in the Raman difference spectra reported below due to its low Raman cross section relative to the preresonance enhancement found in the complex (see below). The procedures for performing the Raman spectroscopy and calculating the Raman difference spectra are discussed in detail elsewhere (10, 11); specific experimental details are given in the figure captions. The resolution in all cases was 8 cm<sup>-1</sup>, band positions are accurate to  $\pm 2 \text{ cm}^{-1}$ , and none of the spectra presented here have been smoothed.

## RESULTS

We have previously discussed some of the features of the Raman spectrum of LDH and those of binary complexes of LDH with NADH, NAD<sup>+</sup>, and adenosine 5'-diphosphate ribose (11). These spectra are dominated by protein bands. The Raman spectrum of the enzyme adduct (LDH/NAD-pyr) contains several new prominent bands. For example, a new band at 1668 cm<sup>-1</sup> appears with a peak intensity about the same as that found for LDH's amide I band. The near-UV spectrum (14) of LDH/NAD-pyr has a small absorption band at 390 nm ( $\epsilon = 2100 \text{ M}^{-1}\text{cm}^{-1}$ ) in addition to the one at 325 nm ( $7700 \text{ M}^{-1}\text{cm}^{-1}$ ). The relatively large intensity observed for the new bands in the LDH/NAD-pyr spectrum is almost certainly due to preresonance enhancement of the Raman cross sections for normal modes associated with this absorption center. The laser lines used to stimulate the Raman scattering in this study are in the blue spectral region, which is sufficiently close enough to cause such an enhancement.

The difference Raman spectrum is obtained by subtracting the LDH protein spectrum from the LDH/NAD-pyr spectrum. The results of this subtraction are shown in Fig. 1, spectrum a, using the protocols described previously (10, 11). To determine the origins of the bands in Fig. 1, spectrum a, as well as to understand the normal mode pattern of the pyruvate adduct in the presence of enzyme and coenzyme, we obtained spectra of the adduct complex with the pyruvate isotopically labeled at different positions. Fig. 1, spectrum b, shows the difference spectrum for the enzyme adduct prepared in H<sub>2</sub><sup>18</sup>O at pH 7.2. The keto oxygen is completely exchanged under these conditions relative to the time needed to prepare the sample. The pronounced band shifts in Fig. 1, spectrum b, relative to Fig. 1, spectrum a, in the region around 1600–1700 cm<sup>-1</sup> substantiate this exchange. Neither the carboxylate oxygens nor the carboxamide oxygen of the cofactor should exchange significantly under these conditions. Fig. 1, spectra c, e, and f, show the difference spectra

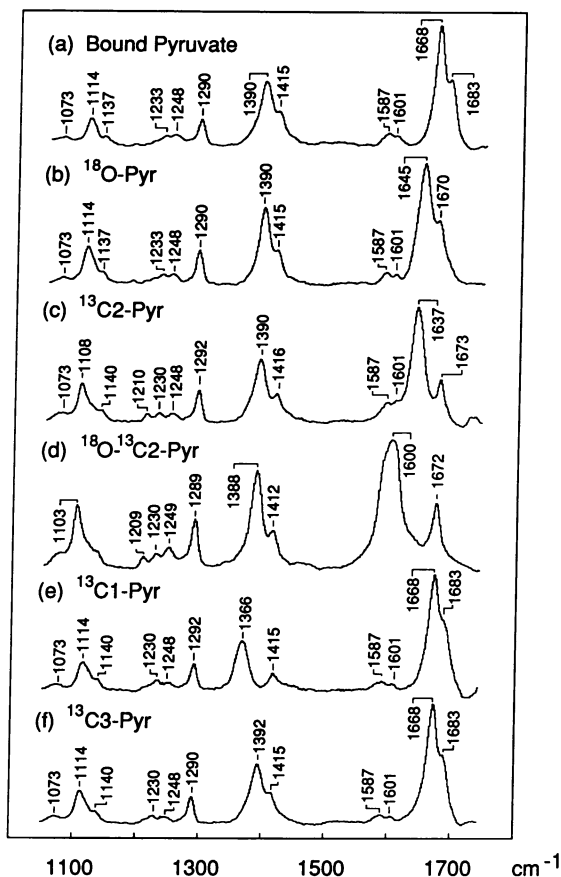


FIG. 1. Raman difference spectra of LDH/NAD-pyr minus LDH in H<sub>2</sub>O (spectrum a), in H<sub>2</sub><sup>18</sup>O (spectrum b), using [2-<sup>13</sup>C]pyruvate (spectrum c), in H<sub>2</sub><sup>18</sup>O and using [2-<sup>13</sup>C]pyruvate (spectrum d), using [1-<sup>13</sup>C]pyruvate (spectrum e), and using [3-<sup>13</sup>C]pyruvate (spectrum f). Spectra a–c were obtained by 457.9-nm laser line and spectra d–f were obtained by 468.0-nm laser line.

of the adduct complex with pyruvate labeled with  $^{13}\text{C}$  at the C2, C1, and C3 positions, respectively. Finally, Fig. 1, spectrum d, was measured for the adduct complex prepared in  $\text{H}_2^{18}\text{O}$  with pyruvate labeled with  $^{13}\text{C}$  at the carbonyl carbon (C2).

Unfortunately, the adduct of pyruvate and  $\text{NAD}^+$  in the absence of enzyme is sufficiently unstable (15) that no spectrum could be obtained. Hence, the Raman spectrum of sodium pyruvate at pH 7.2 is used as a model for the bound pyruvate moiety. This spectrum is shown in Fig. 2 along with the  $^{18}\text{O}$  and  $^{13}\text{C}$  isotopically labeled pyruvates corresponding to those in Fig. 1. The water contribution to these spectra was subtracted, since the major  $1633\text{-cm}^{-1}$  water band is about 30% as intense as the  $1710\text{-cm}^{-1}$  band in Fig. 2, spectrum a, under these conditions.

**Band Assignments.** Pyruvate is a relatively simple molecule with a relatively simple Raman spectrum. The  $1710\text{-cm}^{-1}$  band in Fig. 2, spectrum a, is the carbonyl  $\text{C}=\text{O}$  stretch. This can be seen from its  $32\text{-cm}^{-1}$ ,  $39\text{-cm}^{-1}$ , and  $73\text{-cm}^{-1}$  downward shift upon  $\text{C}^{18}\text{O}$ ,  $^{13}\text{C}=\text{O}$ , and  $^{13}\text{C}^{18}\text{O}$  labeling, respectively (Fig. 2, spectra b–d). These shifts, particularly that resulting from the  $^{13}\text{C}=\text{O}$  labeling, are very close to what would be predicted (41, 38, and  $80\text{ cm}^{-1}$ , respectively) from simple reduced mass calculations on an isolated  $\text{C}=\text{O}$  molecule, which suggests its motion is largely uncoupled from the other motions of the molecule. The  $1398\text{-cm}^{-1}$  and  $1611\text{-cm}^{-1}$  bands are assigned to the symmetric and antisymmetric stretch vibrations, respectively, of the carboxylate,  $\text{COO}^-$ ,

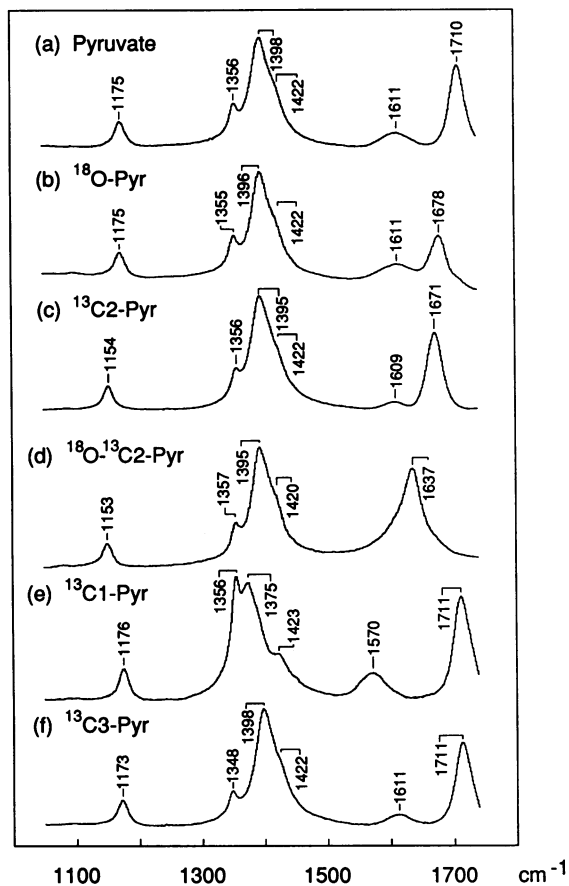


FIG. 2. Raman difference spectra of pyruvate (pH 6.5, 400 mM concentration) minus solvent in  $\text{H}_2\text{O}$  (spectrum a), in  $\text{H}_2^{18}\text{O}$  (spectrum b), using  $[2\text{-}^{13}\text{C}]$ pyruvate (spectrum c) in  $\text{H}_2^{18}\text{O}$  and using  $[2\text{-}^{13}\text{C}]$ pyruvate (spectrum d), using  $[1\text{-}^{13}\text{C}]$ pyruvate (spectrum e), and using  $[3\text{-}^{13}\text{C}]$ pyruvate (spectrum f). Spectra a–c were obtained by  $488.0\text{-nm}$  laser line and spectra d–f were obtained by  $468.0\text{-nm}$  laser line.

group. These bands are in their characteristic positions and disappear upon titrating the  $\text{COO}^-$  group (unpublished data). Moreover, the  $1398\text{-cm}^{-1}$  band shifts to  $1375\text{ cm}^{-1}$  upon  $^{13}\text{C1}$  labeling (Fig. 2, spectrum e), and the  $1611\text{-cm}^{-1}$  band shifts to  $1570\text{ cm}^{-1}$ . The  $1356\text{-cm}^{-1}$  band and the  $1422\text{-cm}^{-1}$  shoulder arise from  $\delta\text{CH}_3$  symmetric and antisymmetric bending motion of the methyl hydrogens. (Note the  $1422\text{-cm}^{-1}$  band becomes evident in Fig. 2, spectrum e, when the  $1398\text{-cm}^{-1}$  band shifts to  $1575\text{ cm}^{-1}$  upon  $^{13}\text{C1}$  substitution). Both the  $1356\text{-}$  and  $1422\text{-cm}^{-1}$  bands remain in the spectrum of protonated pyruvate (unpublished data), and the  $1356\text{-cm}^{-1}$  band moves downward  $8\text{ cm}^{-1}$  to  $1348\text{ cm}^{-1}$  when the  $\text{CH}_3$  group is labeled by  $^{13}\text{C}$  (Fig. 2, spectrum f). The normal mode corresponding to the  $1175\text{-cm}^{-1}$  band of Fig. 2, spectrum a, contains a substantial amount of C2 motion as shown by its  $-21\text{-cm}^{-1}$  shift to  $1154\text{ cm}^{-1}$  upon  $^{13}\text{C}$  labeling of C2 (Fig. 1, spectrum c).

The difference spectrum of the LDH/ $\text{NAD}$ -pyr enzyme adduct of Fig. 1, spectrum a, is considerably more complicated than that of pyruvate. There are more bands, and many of the observed bands do not respond in any significant way to isotopic labeling. Thus, many of the bands cannot be assigned at the present time. The band at  $1668\text{ cm}^{-1}$  is, however, clearly assigned to the  $\text{C}=\text{O}$  carbonyl stretch based on its  $-23\text{-cm}^{-1}$  shift to  $1645\text{ cm}^{-1}$  upon  $\text{C}^{18}\text{O}$  labeling (Fig. 1, spectrum b), its  $-31\text{-cm}^{-1}$  shift to  $1637\text{ cm}^{-1}$  upon  $^{13}\text{C}=\text{O}$  labeling (Fig. 1, spectrum c) and its  $-68\text{-cm}^{-1}$  shift to  $1500\text{ cm}^{-1}$  upon  $^{13}\text{C}^{18}\text{O}$  labeling (Fig. 1, spectrum d). These are large isotope shifts, quite analogous to those observed for pyruvate's carbonyl mode in solution. The  $1390\text{-cm}^{-1}$  peak in Fig. 1, spectrum a, arises from the symmetric  $\text{COO}^-$  stretch as this band shifts to  $1366\text{ cm}^{-1}$  upon  $^{13}\text{C1}$  labeling in Fig. 1, spectrum e. This  $24\text{-cm}^{-1}$  shift is essentially identical to the  $23\text{-cm}^{-1}$  shift we obtained for the symmetric  $\text{COO}^-$  stretch for pyruvate in solution. We note that the  $1356\text{-}$  and  $1422\text{-cm}^{-1}$  bands associated with  $\delta\text{CH}_3$  bending modes in pyruvate in solution are absent in the LDH/ $\text{NAD}$ -pyr enzyme adduct data. This is consistent with the formation of the pyruvate adduct where pyruvate's methyl moiety becomes a  $\text{CH}_2$  group.

Finally, we believe that the  $1683\text{-cm}^{-1}$  band in Fig. 1, spectrum a, contains motions mostly associated with the reduced nicotinamide moiety of the adduct's pyridine ring. This band shifts  $-12\text{ cm}^{-1}$  to  $1670\text{ cm}^{-1}$  upon  $\text{C}^{18}\text{O}$  labeling (Fig. 1, spectrum b) and  $-9\text{ cm}^{-1}$  to  $1673\text{ cm}^{-1}$  upon  $^{13}\text{C}=\text{O}$  labeling (Fig. 1, spectrum c), so this mode is clearly associated with enzyme-bound pyruvate and contains some carbonyl stretching character. However, it is not the carbonyl mode. The frequency shifts upon  $^{18}\text{O}$  and  $^{13}\text{C}$  labeling are much smaller and reversed in their size in comparison to the carbonyl mode of pyruvate in solution at  $1710\text{ cm}^{-1}$  and that at  $1668\text{ cm}^{-1}$  in the enzyme adduct complex. Moreover, there are few other candidates for a mode at this high frequency. The high frequency near  $1683\text{ cm}^{-1}$  suggests the possibility of a  $\text{C}=\text{C}$  stretching motion as such modes are characterized by these frequencies. Finally, a band near  $1680\text{ cm}^{-1}$  is found in the classical Raman spectra of  $\text{NADH}$  (16),  $\text{NAD-CN}$  (unpublished data),  $\text{NAD-pyrazole}$  adducts (10), and  $\text{NADH}$  in LDH (11). The intensities of these modes are similar if not the same as that of the  $1683\text{-cm}^{-1}$  band observed in Fig. 1, spectrum a (as determined by comparing each to LDH's protein band intensity). It is also interesting that the position of the  $1683\text{-cm}^{-1}$  mode in the doubly labeled,  $^{13}\text{C}^{18}\text{O}$ , data found now at  $1672\text{ cm}^{-1}$  (Fig. 1, spectrum d), is unaffected from its position upon  $^{18}\text{O}$  and  $^{13}\text{C}$  labeling found in spectra b and c, respectively. Thus, it seems likely that the  $1683\text{-cm}^{-1}$  mode is associated with the dihydro-like nature of the pyridine ring in the adduct. Some coupling must occur between the pyruvate's  $\text{C}=\text{O}$  stretch and this  $1683\text{-cm}^{-1}$  mode resulting from a resonant interaction due to their near degeneracy

since the frequencies of both bands drop when the carbonyl moiety is labeled by either  $^{18}\text{O}$  or  $^{13}\text{C}$ . This coupling is essentially absent in the labeled compounds since no further frequency change is observed in the pyridine ring mode when the C=O group is doubly ( $^{13}\text{C}=\text{O}^{18}\text{O}$ ) labeled. Hence, for this reason, we have compared below the carbonyl stretch frequency of the doubly labeled adduct complex with that of the doubly labeled pyruvate.

## DISCUSSION

The usefulness of spectroscopic data, such as that given here, is that they yield direct measures of the substrate's electronic configuration at the active site. These data, along with those obtained from both structural studies and computational methods, can provide ultimately a detailed understanding of the forces involved in substrate binding and those leading to catalysis. A moderate-resolution x-ray structure of LDH with bound pyruvate adduct (9) and a refined structure for the E/NADH/oxamate complex (8) are available. We show in Fig. 3 a schematic of the active site of the enzyme/adduct complex with particular attention to pyruvate and its close neighbors as an aid in understanding the results.

There are three main findings from this study. In the first place, the data are consistent with the formation of a covalent bond between the methyl carbon of pyruvate and the C4 position of the pyridinium ring of NAD $^+$ ; this bond has also been suggested on the basis of both structural (7-9) and chemical (15, 17) evidence. The disappearance of pyruvate's  $\delta\text{CH}_3$  band at  $1358\text{ cm}^{-1}$  in the spectrum of the adduct complex is the basis of this conclusion.

The second result is that pyruvate's carboxylate  $\text{COO}^-$  moiety remains unprotonated when it binds to LDH. This is shown by the presence of the  $1390\text{-cm}^{-1}$  band found in the LDH/NAD-pyr data (Fig. 1, spectrum a). This band lies at the characteristic  $\text{COO}^-$  stretching frequency and shifts upon  $^{13}\text{C}$  labeling in the same way that is found in unprotonated pyruvate (Fig. 1, spectrum d). In addition, the frequency of this band is  $8\text{ cm}^{-1}$  lower than that for unbound pyruvate (compare Fig. 1, spectrum a, and Fig. 2, spectrum a, respectively). There are a number of explanations for this lower frequency, including steric effects at the active site that impose conformational constraints on the bound pyruvate. Another explanation, which we favor, involves a system where the protein forms either a somewhat stronger or a more directed hydrogen bonding system with the  $\text{COO}^-$  thus drawing electrons out from the C=O bonds more effectively

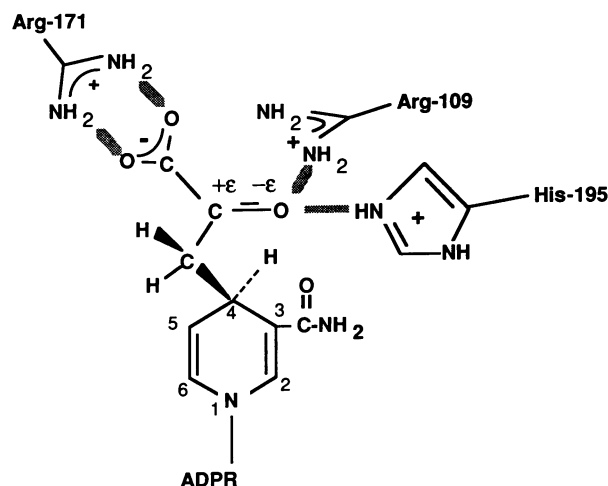


FIG. 3. Drawing, clearly not to scale, of the active site of LDH with NADH and pyruvate based on x-ray results (7-9) and the results presented here (see text). ADPR, adenosine 5'-diphosphate ribose.

than when the carboxylate is "solvated" by water. Such interactions will reduce the symmetrical stretching force constant of the  $\text{COO}^-$ , thereby lowering its frequency. According to the x-ray results (8, 9), Arg-171 form a salt bridge with pyruvate such that its  $-\text{NH}_2^+$  groups are juxtaposed with the oxygens of the carboxylate.

The most dramatic result of this study is the large downward shift in frequency of pyruvate's carbonyl C=O stretching frequency in LDH/NAD-pyr compared to the value for unreacted pyruvate. As discussed in *Results*, there appears to be a small interaction between the C=O moiety and the dihydropyridine ring that only occurs with the unlabeled LDH/NAD-pyr. From the labeled data of Fig. 1, spectra b-d, and Fig. 2, spectra b-d, we calculate that the carbonyl frequency of the bound adduct shifts downward  $34\text{ cm}^{-1}$  relative to that of the unbound pyruvate. As indicated above, this normal coordinate with labeled analogs is highly localized to the carbonyl C=O internal coordinate, and its frequency is a direct indication of the C=O stretching force constant. Hence, this  $34\text{-cm}^{-1}$  decrease in frequency indicates a weakening of the force constant and a decrease in bond order of the C=O of the bound pyruvate adduct relative to that of pyruvate.

This decrease is extremely large. Its size may be estimated by considering that acetone's C=O stretching frequency decreases  $99\text{ cm}^{-1}$  when it is fully protonated (18). Our effect is some 34% of that for a fully protonated species, which suggests that the bound carbonyl bond has substantially more single bond character than the unbound carbonyl. This conclusion is also reached by noting that the frequencies of amide I bands in proteins, around  $1660\text{ cm}^{-1}$ , are essentially the same as that we have found for the bound pyruvate adduct. The amide I normal mode consists largely of the stretch of polypeptide backbone C=O group. However, its low frequency arises from  $\pi$  electron resonance effects between the C=O moiety and the backbone C-N bond that substantially reduces the C=O bond order. From x-ray data, it has been estimated that the C=O bond order is about three parts double bond and two parts single bond (19).

Substantial C=O bond polarization has been detected for substrates bound to other enzymes as well. For instance, Belasco and Knowles (20, 21), by Fourier transform IR spectroscopy, have detected decreases of 19% and 23% for triosephosphate isomerase and aldolase, respectively. In addition, Kurz *et al.* (22), by  $^{13}\text{C}$  NMR studies, found carbonyl bond polarization of about 20-30% in oxaloacetate bound to citrate synthase. Finally, the C=O of the aromatic aldehyde, *p*-(dimethylamino)benzaldehyde (DABA), when bound at the catalytic site of liver alcohol dehydrogenase (12), is substantially polarized as well. The frequency of the C=O stretch is  $1644\text{ cm}^{-1}$  for DABA in water and shifts to around  $1550\text{ cm}^{-1}$  when DABA is bound to LADH. This *ca.*  $94\text{-cm}^{-1}$  shift cannot be directly compared to that observed for LDH since DABA's  $\pi$  electron structure is highly delocalized, which causes the mode associated with DABA's aldehyde bond to be highly extended, unlike that of the pyruvate adduct. For example, DABA's carbonyl frequency lies at  $1695\text{ cm}^{-1}$  in the aprotic solvent diethyl ether and at  $1644\text{ cm}^{-1}$  in water, a shift of  $51\text{ cm}^{-1}$  due to differences in the electrophilic properties of these solvents. By comparison, acetone's C=O normal mode shifts  $10\text{ cm}^{-1}$  when acetone is transferred from acetone to water (unpublished data). Thus, crudely, DABA's C=O mode shifts  $5\text{ cm}^{-1}$  for every  $1.0\text{ cm}^{-1}$  observed for acetone and, presumably, other simple ketones like pyruvate. Correcting the C=O shift observed for DABA in water to that observed for LADH by this "normalizing" factor, we find an "equivalent" shift of  $19\text{ cm}^{-1}$ , which then is more directly comparable to pyruvate's  $34\text{-cm}^{-1}$  shift. Thus substantial bond polarization of simple aldehydes may also occur at the active site of LADH.

The electrophiles giving rise to the C=O bond polarization in LDH almost certainly involve the imidazole group of His-195 and the guanidino groups of Arg-109 and possibly Arg-171, since x-ray studies (7, 9) place the first two of these residues close to the oxygen of the carbonyl moiety and the latter is ion paired with the carboxylate of pyruvate (Fig. 3). In addition, Clarke *et al.* (23, 24) have detected significant interactions between Arg-109 and the carbonyl by site-directed mutagenesis. On the other hand, LADH accomplishes a similar C=O aldehyde bond polarization with an entirely different molecular environment. Here, the positively charged molecular factor is inorganic Zn<sup>2+</sup>, which is liganded to three protein residues. The fourth ligand is the substrate whose spectroscopic molecular properties are virtually the same as Zn-substrate complexes in hydrophobic solvents (12). This indicates a strong interaction between DABA and Zn<sup>2+</sup> at LADH's active site that is typical of ligands of metal cations in cation-metal complexes. Since the polarization of pyruvate's carbonyl bond is similar, the pyruvate-LDH interaction must be similarly strong.

At least three different factors in the rate acceleration accomplished by LDH have been independently characterized on the basis of analog reactions (4). One of us (J.B.) has suggested (4) that these effects, which consist of factors of 10<sup>2</sup>-fold due to environmental changes that occur during the formation of the LDH/NAD<sup>+</sup> binary complex, of 10<sup>3</sup>-fold due to immobilization of reactants at the active site, and of 10<sup>6</sup>-fold due to the general base-catalyzed addition of *enol*-pyruvate to NAD<sup>+</sup>, entirely account for the 10<sup>11</sup>-fold rate effect observed with the adduct reaction. Certainly, the large polarization that we have observed here is consistent with the unexpectedly large rate effect noted for general base catalysis. In addition, we have shown here that pyruvate interacts strongly with the protein through specific electrostatic factors at both its carboxylate and carbonyl groups, and these interactions are likely sufficient to account for immobilizing this reactant at the active site. This set of interactions also implies binding of pyruvate with a specific geometry. We have recently observed strong hydrogen bonding patterns between NAD's carboxamide group and the enzyme in vibrational studies similar to those reported here (11), which, together with other interactions, should be sufficient to fix the orientation of the coenzyme at the active site. Whether this restrictive environment is completely responsible for the high fidelity (5) of the hydride stereochemical transfer, approaching 100% (99.999997) is not yet known. Finally, bond polarization of pyruvate's C=O moiety leads to positive charge accumulation on pyruvate's C2 carbon, making this carbon much more susceptible to hydride attack. Moreover, the strong positively charged environment around the carbonyl oxygen would stabilize the polar <sup>+</sup>C—O<sup>-</sup> transition state associated with the pyruvate to lactate transition.

This work was supported by Grants GM35183 (City College) and RCMI Grant RRO3060 (City College) from the National Institutes of Health and by Grant 8616216 from The National Science Foundation (Purdue University).

1. Jencks, W. P. (1986) in *Proceedings of the XVII Solvay Conference on Chemistry*, ed. Van Binst, G. (Springer, New York), pp. 59–80.
2. Wolfenden, R. (1976) *Annu. Rev. Biophysics Bioeng.* **5**, 271–306.
3. Fersht, A. (1985) *Enzyme Structure and Mechanism* (Freeman, New York), pp. 47–94.
4. Burgner, J. W., II & Ray, W. J., Jr. (1984) *Biochemistry* **23**, 3636–3648.
5. Anderson, V. E. & LaReau, R. D. (1988) *J. Am. Chem. Soc.* **110**, 3695–3697.
6. Burgner, J. W., II & Ray, W. J., Jr. (1984) *Biochemistry* **23**, 3620–3626.
7. Holbrook, J. J., Lijas, H., Steindel, S. J. & Rossmann, M. D. (1975) in *Enzymes*, ed. Boyer, P. D. (Academic, New York), 3rd Ed., pp. 191–292.
8. White, J. L., Hackert, M. L., Buehner, M., Adams, M. J., Ford, G. C., Lentz, P. J., Jr., Smiley, I. E., Steidel, S. J. & Rossmann, M. G. (1976) *J. Mol. Biol.* **102**, 759–779.
9. Grau, U. M., Trommer, W. E. & Rossmann, M. G. (1981) *J. Mol. Biol.* **151**, 289–307.
10. Chen, D., Yue, K. T., Martin, C., Rhee, K. W., Sloan, R. & Callender, R. H. (1987) *Biochemistry* **26**, 4776–4784.
11. Deng, H., Zheng, J., Sloan, D., Burgner, J. & Callender, R. H. (1989) *Biochemistry* **28**, 1525–1533.
12. Callender, R. H., Chen, D., Lugtenburg, J., Martin, C., Rhee, K. W., Sloan, D., Vandersteen, R. & Yue, K. T. (1988) *Biochemistry* **27**, 3672–3681.
13. Burgner, J. W., II & Ray, W. J. (1978) *Biochemistry* **17**, 1654–1661.
14. Burgner, J. W., II & Ray, W. J. (1974) *Biochemistry* **13**, 4229–4237.
15. Everse, J., Barnett, R. E., Thorne, C. J. R. & Kaplan, N. O. (1971) *Arch. Biochim. Biophys.* **143**, 444–460.
16. Yue, K. T., Yang, J.-P., Martin, C. L., Lee, S. K., Sloan, D. L. & Callender, R. H. (1984) *Biochemistry* **23**, 6480–6483.
17. Ozols, R. F. & Marinetti, G. V. (1969) *Biochem. Biophys. Res. Commun.* **34**, 712–714.
18. Clemett, C. J. (1970) *J. Chem. Soc. D*, 211–212.
19. Schulz, G. E. & Schirmer, R. H. (1979) *Principles of Protein Structure* (Springer, New York), pp. 18–20.
20. Belasco, J. G. & Knowles, J. R. (1980) *Biochemistry* **19**, 472–477.
21. Belasco, J. G. & Knowles, J. R. (1983) *Biochemistry* **22**, 122–129.
22. Kurz, L. C., Ackermann, J. J. H. & Drysdale, G. R. (1985) *Biochemistry* **24**, 452–457.
23. Clarke, A. R., Wigley, D. B., Chia, W. N., Barstow, D. A., Atkinson, T. & Holbrook, J. J. (1986) *Nature (London)* **324**, 699–702.
24. Clarke, A. R., Wilks, H. M., Barstow, D. A., Atkinson, T., Chia, W. N. & Holbrook, J. J. (1988) *Biochemistry* **27**, 1617–1622.